ELSEVIER

Chemical Engineering Science 62 (2007) 3984–3990

Chemical Engineering Science

www.elsevier.com/locate/ces

CO oxidation over structured carriers: A comparison of ceramic foams, honeycombs and beads

Florina Corina Patcas*, Gerardo Incera Garrido, Bettina Kraushaar-Czarnetzki

Institute of Chemical Process Engineering CVT, University of Karlsruhe, Kaiserstrasse 12, D-76128 Karlsruhe, Germany

Received 10 January 2007; received in revised form 30 March 2007; accepted 27 April 2007
Available online 10 May 2007

Abstract

This work aims an experimental comparison of different packings on the basis of their pressure drop, mass and heat transfer properties. Ceramic foams, beads and a honeycomb monolith were used as carriers in the oxidation of carbon monoxide. The carriers were coated with active Pt/SnO_2. The CO oxidation rate was measured in the regime of external diffusion control at superficial gas velocities between 1 and 10 m/s. The volumetric rate coefficients and the pressure drop of packings with similar geometric surface area decreased in the sequence particles > foams > honeycomb. The magnitude of the temperature gradient along the catalytic bed decreased as going from honeycomb over larger particles to foams and small particles. Foams were superior over particle beds from the viewpoint of combined high mass transfer and low-pressure drop. The main advantage of foams as compared to honeycomb resided in the radial mixing enabling a better heat transfer to the reactor walls.

Keywords: Ceramic foam; Structured catalyst; Mass transfer; Heat transfer; Pressure drop; Catalyst support

1. Introduction

Monolithic honeycomb carriers have found a large application field in the environmental area, because of their low-pressure drop. They did not manage, however, to penetrate the industrial production owing to some limitations such as the poor heat transfer and the lack of radial mixing (Groppi et al., 2006; Heck et al., 2001). In the last few years monolithic ceramic or metal foams came increasingly into attention as a new type of low-pressure drop carriers. The heat and mass transfer properties of foams have been scarcely investigated and the few literature data are still controversial (Giani et al., 2005; Richardson et al., 2003; Younis and Viskanta, 1993). Based on the very particular structure and morphology of foams there is much hope regarding a better tradeoff between the low-pressure drop, characteristic to honeycomb carriers, and the high mass and heat transfer properties of particle packings. This work aims to investigate comparatively the oxidation of carbon monoxide over ceramic foams, honeycomb monolith and bead packings of similar external surface areas coated with Pt/SnO_2 as an active phase. This reaction is used here mainly as a tool to determine the mass transfer coefficients of the carriers, but it is also an interesting subject by itself due to the increased interest in the purification of hydrogen gas for fuel cells. The synergy between Pt and SnO_2 leads to a high CO oxidation activity at moderate temperatures and tolerance against CO and water poisoning (Grass and Lintz, 1995; Schryer et al., 1991).

Honeycomb monoliths are composed of regularly arranged parallel channels (Heck et al., 2001). The most important characteristics are the channel size, expressed as channel per square inch (cpsi), and the open frontal area, which amounts to 63–87% (ceramic bodies) and to ca. 90% (metallic bodies). The main advantages of honeycombs reside in their low-pressure drop, high-geometric surface, robustness, strength and low weight (Cybulski and Moulijn, 1994). The ceramic monoliths are operated essentially adiabatically, because of their low thermal conduction and the lack of radial mixing that yield a poor heat transfer to the walls.

Foam monoliths can be made of ceramic or metal. The open cell foams consist of a network of interconnected solid struts

* Corresponding author. Tel.: +49 721 608 4134; fax: +49 721 608 6118.
E-mail address: Florina.Patcas@ciw.uni-karlsruhe.de (F.C. Patcas).

0009-2509/$ - see front matter © 2007 Elsevier Ltd. All rights reserved.
doi:10.1016/j.ces.2007.04.039

building cavities (=cells) that communicate through windows. Ceramic foams have open porosities of 75–85% and the metallic foams of about 95%. The main characteristic is the size of pores, which is usually expressed as the pore count "pores per inch" (ppi). Commercial foams have pore counts between 5 and 100 ppi. The structure of foams allows low-pressure drop flowing with radial mixing, tortuous flow paths and enhanced turbulence in the pores. The heat transport to the walls occurs not only by conduction, as in honeycombs, but also by convection and radiation.

The present attempt to compare these two types of low-pressure drop carriers with conventional spherical particles is based on direct experimental data and is, as far as the authors are aware, unique. The only similar evaluation until now was based on a mixture of measured data and literature correlations (Giani et al., 2005). Here a tradeoff index was defined, based on the volumetric conversion rate and the friction factor, to allow the quantitative comparison of different carriers. The calculated tradeoff indexes decreased in the sequence honeycomb $\geqslant$ foam $>$ spheres. In our work we measure the effective volumetric rate coefficients and pressure drops in the external diffusion controlled kinetic regime. To allow the comparison on a mutual basis, carriers of similar volumetric surface areas were employed.

2. Experimental

2.1. Selection and characterization of carriers

Foam monoliths having 20 and 45 ppi were compared with square-channel honeycomb monoliths with 400 cpsi on the basis of similar pore/channel count (20 ppi–400 cpsi) or surface area (45 ppi–400 cpsi), respectively. The criterion for the choice of the beads carriers was the geometric surfaces that were close to those of the foams. The 20 and 45 ppi foams were compared with beads of 3.3 and 1.5 mm, respectively. Fig. 1 shows a snapshot of some of the employed carriers.

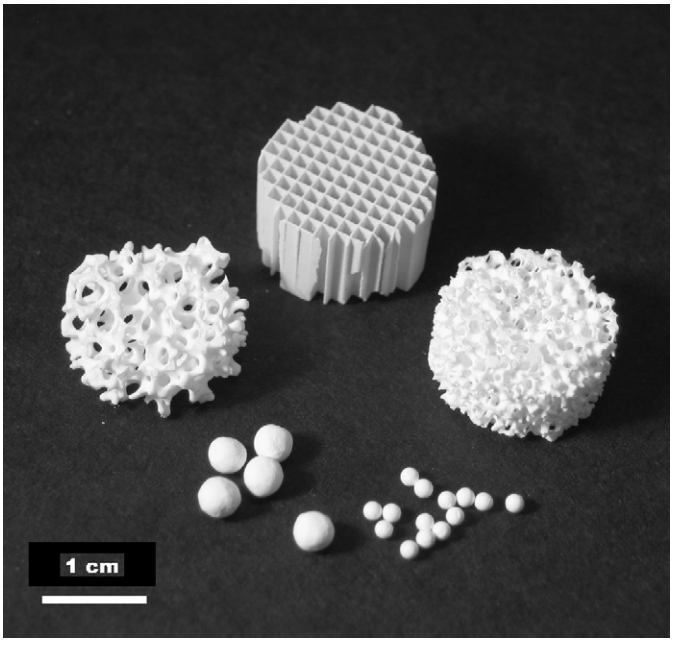

Fig. 1. SnO_2-coated ceramic carriers: 20 and 45 ppi foams, 400 cpsi honeycomb, 3.3 and 1.5 mm beads.

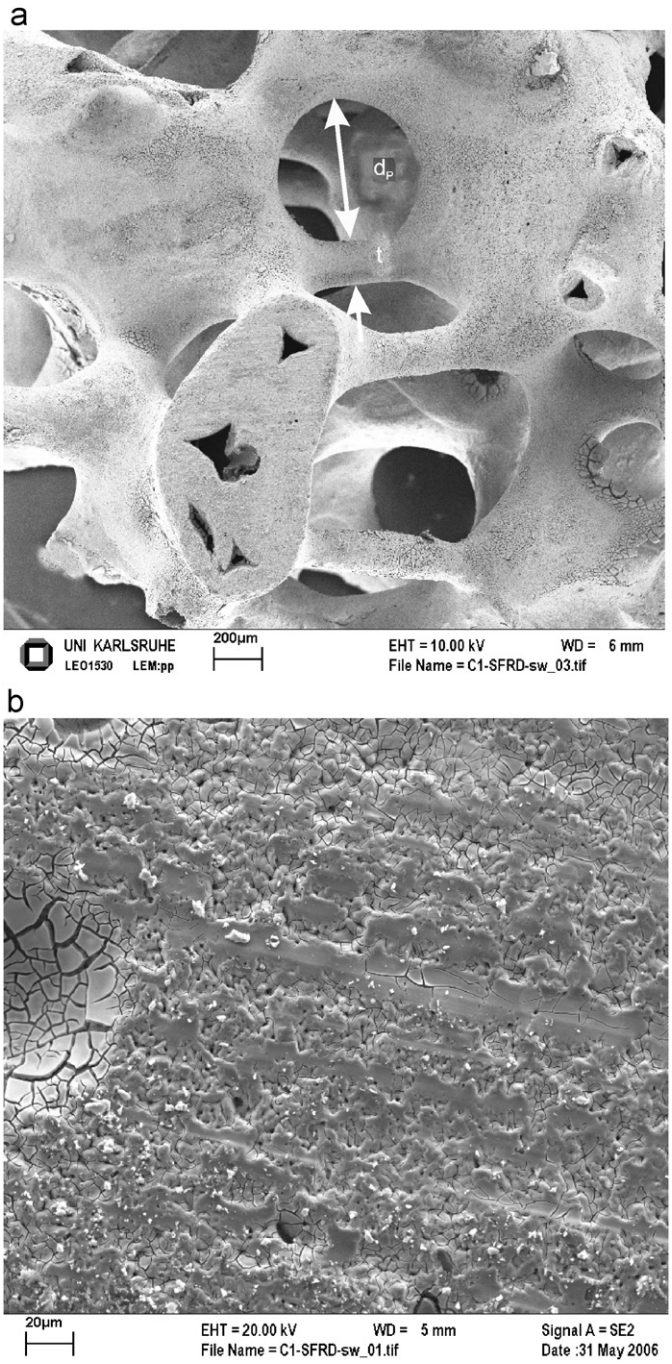

Fig. 2. Scanning electron microscopy images of the SnO_2 coated 45 ppi alumina foam: (a) overview of morphology features "pore diameter" d_P and "strut thickness" t; (b) top view of the SnO_2 coat.

The ceramic foams were made of α-alumina by HighTech Ceramics. The honeycomb was made of cordierite by Corning. The beads were from Norton and made of α-alumina. Both foam and honeycomb monoliths were cut in cylinders of 15 mm

Table 1
Properties of ceramic carriers after coating

Carrier	Char. size d_P (mm)	Strut/wall thickness t (mm)	Bed density (kg/m^3)	Solid density (kg/m^3)	Bed porosity (%)	Geometric surface area (m^2/m^3)
Foam 20 ppi	1.19	0.42	829	3157	73.7	1535
Foam 45 ppi	0.68	0.20	794	3200	75.2	2728
Honeycomb 400 cpsi	1.12	0.21	480	1660	70.9	2530
Beads 3.3 mm	3.33	–	764	1365	44.0	997
Beads 1.5 mm	1.45	–	1259	2134	41.1	2436

diameter before coating. All carriers were precalcined before coating in order to remove organic contaminants. The carriers were coated by repeatedly dipping them in a 20 wt% SnO_2-sol, draining, drying and heating at 350 °C. To achieve a uniform, continuous SnO_2 coat of ca. 5 μm thickness, about 5–10 wt% loading depending on the geometric area and roughness of the carrier was required. A picture of the coated 45 ppi foam, together with a magnification showing the SnO_2 top layer, is shown in Fig. 2.

Some characteristics of the SnO_2-coated carriers are presented in Table 1. The bed density was calculated by using the weight and volume of bed. The packing porosity and solid (strut) density of foams were determined by pycnometry using mercury as a non-wetting fluid. For the honeycomb manufacturer data for density and porosity were taken and corrected for the weight and volume of the coat. For beads the average solid density was measured for 30 coated particles. The characteristic sizes in Table 1 are the average pore diameter (foams), channel size (honeycomb) and particle diameter (beads). The average pore diameter of the coated foams d_P (a pore being the window between two cells, see Fig. 2a) and the strut thickness t were determined with a light microscope by using 300 features in each case. The geometric surface area of foams was calculated on the basis of a tetrakaidekahedron model (Buciuman and Kraushaar-Czarnetzki, 2003). The channel size and wall thickness of the coated honeycomb monolith were also measured microscopically, then the geometric surface area was calculated according to Cybulski and Moulijn (1994).

2.2. Loading with Pt and activation

Platinum was loaded by using the supercritical fluid reactive deposition (SFRD) method. Therefore, the SnO_2-coated carriers were placed into a pressure vessel together with the organic platinum complex Pt(COD)Me$_2$ (dimethyl-1,5-cyclooctadienplatinum). The complex was dissolved in scCO_2 at 80 °C and 15.5 MPa and allowed in these conditions to adsorb on the SnO_2 phase for 20 h. The adsorbed complex was subsequently decomposed by adding H_2 at isothermic and isobaric conditions for 2 h, leaving only reduced Pt on the catalyst. After depressurization the Pt/SnO_2/carrier catalyst was already in the activated (reduced) form. The amount of complex in the autoclave was preset such as to attain about 10% (wt) Pt relative to the SnO_2 coat. The platinum content of the catalyst was determined gravimetrically. This method allows a very homogeneous and fine dispersion of platinum nanoparticles on the surface of SnO_2.

2.3. Kinetic tests of CO oxidation

The CO oxidation rates were measured in a tubular gradientless, electrically heated glass reactor with external recycling by a membrane pump. To ensure a good mixing the recycle ratio was kept at 25–30. The volumetric flow of the membrane pump could be varied in order to achieve different flow rates within the reactor. The catalytic bed was placed in the center of the reactor. Up- and downstream to the catalyst, blank carrier beds of the same type, each in length of 20 mm were placed in the reactor, to build and stabilize the characteristic fluid stream. In the case of the honeycomb carrier, care has been taken to ensure the perfect continuity of the channels, in order to avoid turbulences at the entrance and outlet of the catalytic middle piece. The monoliths were sealed with quartz fabric against the reactor wall. Thermocouples were directly inserted in the reactor at the entrance and outlet of the catalyst bed by means of two lateral glass tubes, which also enabled the measurement of the pressure drop by a water manometer.

The reaction rate relative to the catalyst bed volume was calculated by mass balancing the open CSTR system in the steady state as follows:

$$r = \frac{C_{0,\mathrm{CO}} X \dot{V}_0}{V_{\mathrm{cat}}}. \quad (1)$$

The inlet gas mixture contained low concentrations (0.05–0.40 vol%) of CO in air. The concentrations of CO and CO_2 at the entrance and outlet of the recycle loop were measured with a non-dispersive IR photometer (BINOS, Fisher-Rosemount).

3. Results and discussion

3.1. Catalyst characterization

The SnO_2 coat was examined via scanning electron microscopy (SEM) to assess its quality and continuity. Fig. 2 shows exemplarily SEM pictures of the surface of a SnO_2-coated 45 ppi foam. The bare carriers have generally a coarse surface but the SnO_2 coat, being composed of nanometer particles, is very smooth. The platinum loading does not change the aspect of the SnO_2-coated carriers, the noble metal being

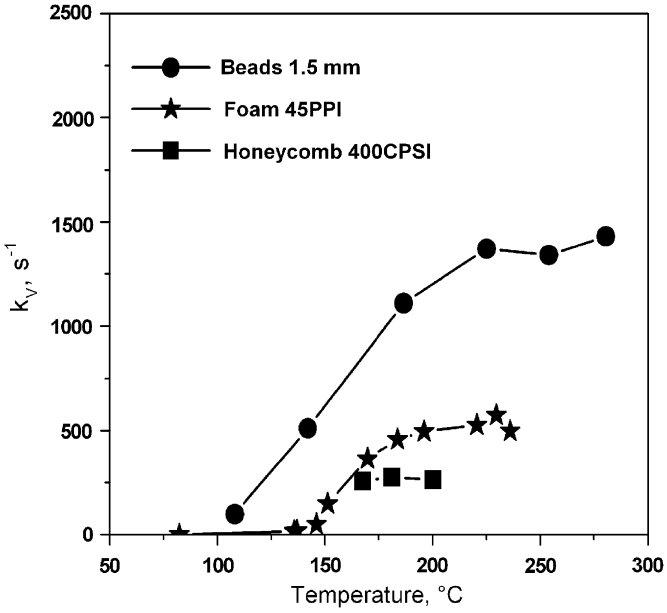

Fig. 3. Estimation of the mass transfer controlled temperature range: first order volumetric rate constant as a function of bed temperature at a superficial velocity of 9 m/s.

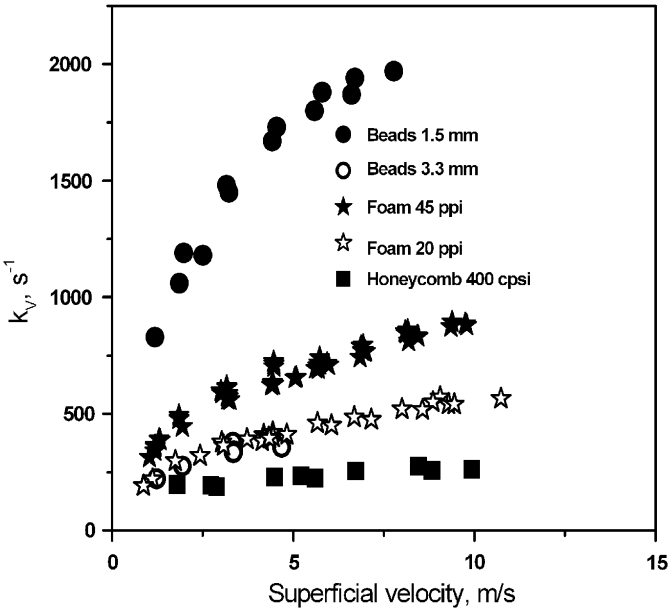

Fig. 4. Volumetric rate constants as a function of the superficial gas velocity over different carriers in the mass transfer controlled kinetic regime.

very finely divided. The microscopic inspection of all carriers showed a continuous, uniform coating with active phase.

3.2. Carbon monoxide oxidation and external mass transfer

The kinetic measurements were performed by using superficial gas velocities in the range of 1–10 m/s (reactor conditions).

For each catalyst packing the first step was to find the temperature range where the oxidation rate was controlled by the external mass transfer at the highest flow rate. Fig. 3 shows exemplarily the evolution of the first-order kinetic rate constant (Eq. (2)) with the average packing temperature over three different packings. The data were measured at a superficial gas velocity of about 9 m/s. Because the mass transfer coefficients increase with increasing flow rate, a process that is diffusionally controlled at 9 m/s will be more so at lower flow rates. The transition from the kinetic to the diffusion-controlled regime, shown by the very weak rate dependence on temperature, took place, depending on the magnitude of the individual mass transfer coefficients, at different temperatures. Thus, over honeycomb the process was diffusion controlled already at 150 °C, whereas over 45 ppi foam this range began at about 200 °C and over 1.4 mm beads at 250 °C. The following experiments were consequently performed at 170–180 °C (honeycomb), 210–220 °C (foams) and 250–260 °C (beads), that is, in the mass transfer controlled temperature range.

$$r = k_V C_{CO}. \tag{2}$$

The first-order kinetic constants based on the bed volume, k_V, as a function of the superficial gas velocity are shown in Fig. 4. Full symbols denominate carriers with about 2500 m^2/m^3 surface area and open symbols those with 1000–1500 m^2/m^3. The constants k_V are proportional to the mass transfer coefficients k_m and the geometric surface areas S_V of the respective carriers after

$$k_V = k_m S_V. \tag{3}$$

In the series 45 ppi foam–400 cpsi honeycomb–1.5 mm beads a definite trend is recognizable in the ranking of the external mass transfer coefficients, namely, beads > foam > honeycomb. The honeycomb displays actually the poorest performances with respect to the CO oxidation among all carriers tested. The performances of the 20 ppi foam and 3.3 mm beads are sensibly equal, which can be accounted for by the fact that the bed surface area of the beads is lower than that of the foam (Table 1). To ascertain the quality of the experiments and to validate the correctness of the mass transfer coefficients, a comparison of the measured data with literature correlations of well-known packings is displayed in Fig. 5. In the definition of the *Re* number the characteristic sizes d_P from Table 1 were employed. As Fig. 5 shows, there is a very good fit between experimental datapoints and the correlation of Dwivedi and Upadhyay (1977) for spherical particles beds (Eq. (4)) and of Hawthorn for honeycomb monoliths (Eq. (5)) (Cybulski and Moulijn, 1994):

$$\varepsilon j_D = 0.4548 Re^{-0.4069}, \tag{4}$$

$$Sh = 2.976\left(1 + 0.078 Re\, Sc \frac{d_P}{L}\right)^{0.45}. \tag{5}$$

Eq. (4) was adapted to the *Sh–Re* representation by using

$$Sh = j_D Re\, Sc^{1/3}. \tag{6}$$

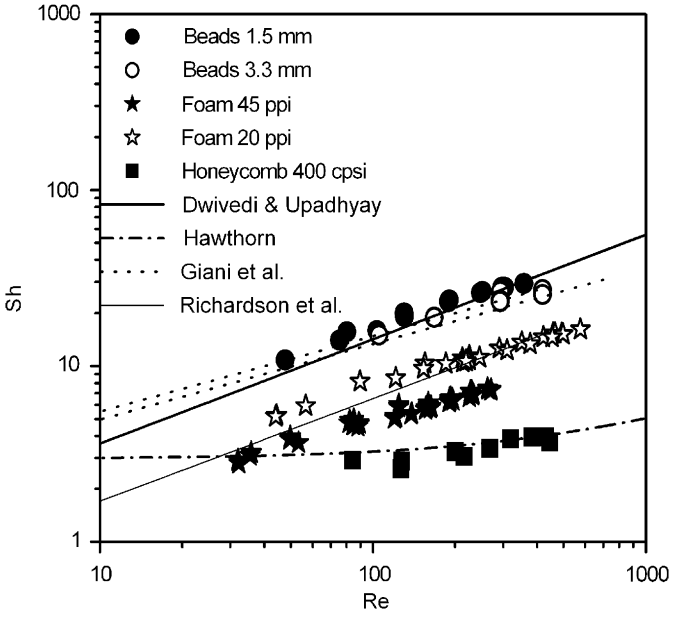

Fig. 5. Experimental data (points) vs. literature correlations (lines) for different carriers.

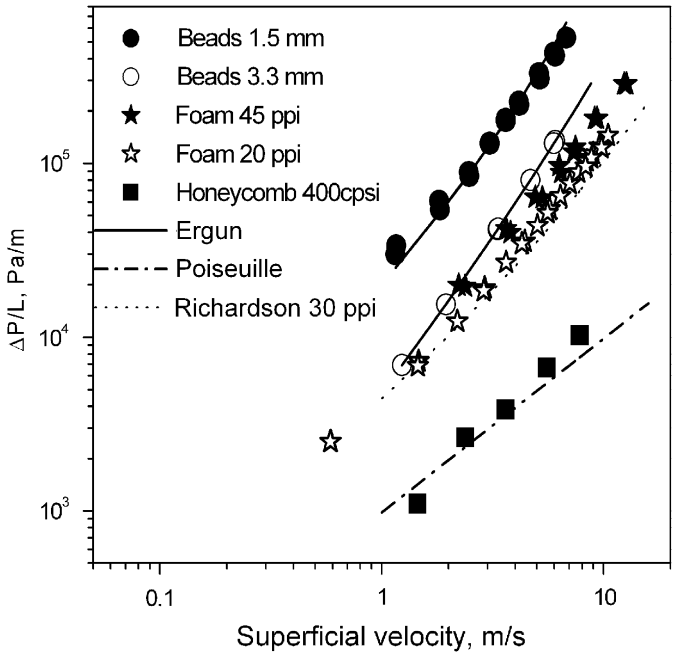

Fig. 6. The pressure drop as a function of the superficial gas velocity at reaction conditions. The lines are calculated values after Eqs. (9)–(11).

For the sake of comparison, foam bed correlations given by Richardson et al. (2003) (Eq. (7)) and by Giani et al. (2005) (Eq. (8)), adapted to our definitions of *Re* and *Sh*, are also shown in Fig. 5. In the work of Richardson et al. the characteristic length for the definition of *Re* was the reciprocal surface area, whereas in the work of Giani et al. the characteristic size was the strut thickness:

$$\varepsilon j_D = 0.233 Re_S^{-0.416}, \tag{7}$$

$$Sh = 1.1 Re^{0.43} Sc^{1/3}. \tag{8}$$

The equation of Richardson et al. was calculated for their 30 ppi foam data and falls well between our measured data for 20 and 45 ppi foams. The equation of Giani et al. (the lines in Fig. 5 were calculated using morphological data of our 20 and 45 ppi foams) gives much larger mass transfer coefficient data. Here it should be observed that the porosities of our (coated) foams were generally lower than those of Richardson et al. (ca. 82%) and much lower than those of Giani et al. (ca. 94%). This could be the reason for the better coincidence of our measured data with the Richardson's correlation, than with the correlation of Giani et al. Apparently the influence of porosity on the mass transfer coefficients is larger than estimated within previous studies, which indicates that for the establishment of reliable correlations the porosity of foams should be varied in a broader range.

An interesting observation derived from Fig. 5 is that the *Sh–Re* lines for foams of different pore counts (20 and 45 ppi) are definitely apart. One reason could be the improper choice of the characteristic size; instead of the window diameter, the strut diameter could be used, as already done by Giani et al. Alternatively a further dimensionless group including the characteristic size of the foam (e.g., the window diameter) could be included in the *Sh–Re* correlations to bring all foams on a common trend line. Our future work will explore both possibilities using foams with a broad range of pore counts.

3.3. Pressure drop

The pressure drop at different superficial velocities was measured at the reaction temperature in the open loop. The data points are presented together with theoretical estimations (lines) in Fig. 6. For beads the Ergun equation was used:

$$\frac{\Delta P}{L} = \frac{150\eta(1-\varepsilon)^2}{d_P^2\varepsilon^3} w_0 + \frac{1.75\rho(1-\varepsilon)}{d_P\varepsilon^3} w_0^2, \tag{9}$$

while for honeycomb the pressure drop was calculated with the Hagen–Poiseuille equation (Cybulski and Moulijn, 1994):

$$\frac{\Delta P}{L} = \frac{32\eta}{d_P^2\varepsilon} w_0. \tag{10}$$

In Fig. 6 an estimation of the pressure drop in a 30 ppi foam after Richardson et al. (2000) is also presented

$$\frac{\Delta P}{L} = 3790 w_0 + 651 w_0^2. \tag{11}$$

The pressure drop calculated after Richardson is somewhat lower that the values measured by us on foams, but one must consider that the foams of Richardson had a higher porosity (around 87%) than our both foams (see Table 1), so in this respect our measured values agree satisfactorily with Richardson's.

By examining Fig. 6 one sees that the magnitude of the pressure drop for carriers having the same surface area displays the same trend as the mass transfer coefficients, namely, beads > foam > honeycomb.

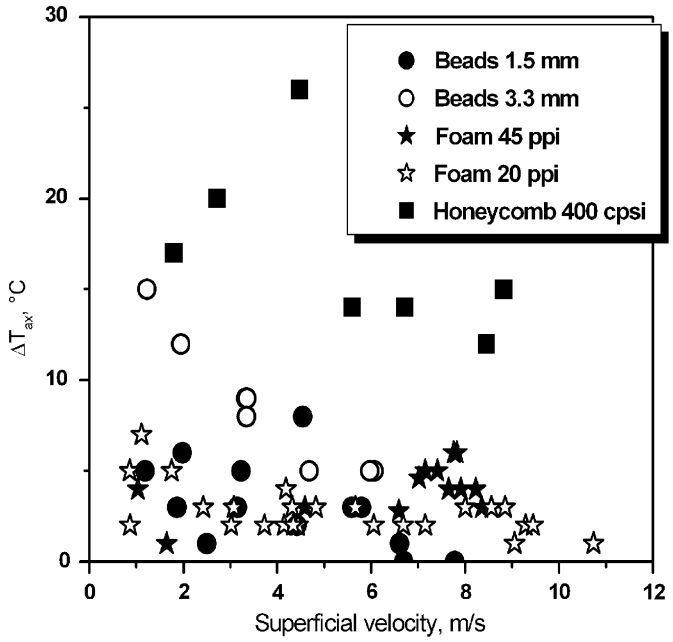

Fig. 7. The temperature increase along the catalyst bed during CO oxidation at comparable conversions per pass.

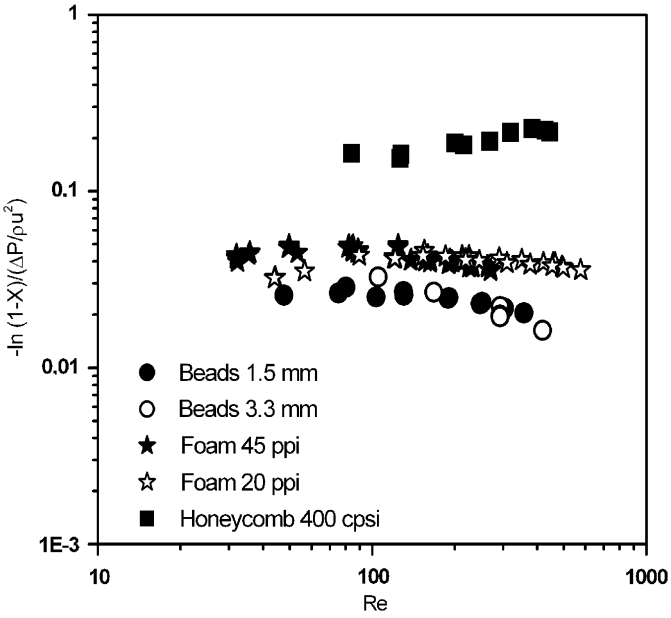

Fig. 8. A comparison of experimental tradeoff indexes (Eq. (12)) as a function of the *Re* number for the particles, foams and honeycomb packings.

3.4. Axial temperature gradient

The differences between the inlet and outlet temperatures of the gas in the CO oxidation reactor, at comparable CO conversion grades on different carriers, are shown in Fig. 7. One sees that both 20 and 45 ppi foams display the lowest temperature gradients, of the same magnitude as the smallest beads packing (1.5 mm). This points to a good radial heat transfer within foam beds, which relies on the unique combination of full radial gas mixing and fast heat conduction through the continuous struts network. In the case of the bigger particles (3.3 mm beads) the fewer contact points between particles produce poorer heat conduction. The honeycomb monolith displays as expected by far the largest temperature gradients because of the total lack of radial mixing.

3.5. Assessment of the carrier performances as a catalytic packing

Since the permeability and mass transfer capability of the carriers are opposite, it is difficult to decide which carrier is more advantageous from the viewpoint of a maximal mass transfer at a minimal pressure drop. Therefore we use the combined performance parameter defined by Giani et al. (2005) as the "dimensionless tradeoff index":

$$I = \frac{-\ln(1-X)}{\Delta P/(\rho w_0^2)}, \tag{12}$$

X being the fractional conversion and ΔP the pressure loss achieved along a bed of length L at a superficial velocity w_0 in the mass transfer controlled kinetic regime. This index has the advantage of being dependent only on the bed geometry and not on the characteristic size within a certain packing type (Giani et al., 2005). A large index means high reaction rates at simultaneous low-pressure drop. The calculated values of the tradeoff index on the basis of our experimental data are shown in Fig. 8.

According to Fig. 8 the honeycomb monolith is the most advantageous from the viewpoint of combined conversion and permeability, followed by the foam monolith and the particle packing. In the work of Giani et al. the foam packing was almost equal to the honeycomb with respect to the tradeoff index. At any rate, the foam performs better than beads packing. The other aspect to be considered is the heat transfer within the bed. Most reactions that are performed at short contact times, where the magnitude of the mass transfer is important for the kinetics, are also highly exothermal. In many processes like the partial oxidations the temperature plays a decisive role in the control of selectivity and lifetime of the catalyst. Here the foams and the spherical beads outrun the honeycomb obviously, as the data in Fig. 7 show. The foams appear to be in fact better in heat transfer than the beads. Consequently the foams seem to offer the best tradeoff between a high mass transfer, permeability and heat transfer among the tested catalytic packings.

4. Conclusions

Catalytic foam packings combine a high permeability to gas flow with good mass and heat transfer characteristics. Their pressure drop and mass transfer coefficients are between those of particles packings and honeycomb monoliths. The heat transfer within foams is very efficient, being comparable with that of small particle beds. Compared to particle packings, foams ensure a better mass transfer/pressure drop tradeoff. Compared to honeycomb monoliths, foams offer the advantage of radial

mixing and more efficient heat transfer. For these reasons the foam monoliths may become an attractive alternative to particle packings and honeycomb monoliths in applications such as gas pollution, on-board hydrogen production and the industrial chemical synthesis.

Notation

$C_{0,\mathrm{co}}$	inlet CO concentration, mol/m^3
C_{eo}	CO average concentration in reactor, mol/m^3
d_P	characteristic size, m
D_{CO}	molecular diffusion coeficient of CO, m^2/s
k_m	mass transfer coefficient gas/solid, m/s
k_V	apparent first order rate constant based on bed volume, s^{-1}
L	bed length, m
ΔP	pressure drop, Pa
r	reaction rate, mol/m^3 s^1
S_V	geometric surface area, m^2/m^3
t	strut (wall) thickness, m
V_{cat}	catalyst bed volume, m^3
$\dot{V}_0$	volumetric inlet flow, m^3/s
w_0	superficial velocity, m/s
X	conversion grade, dimensionless

Greek letters

ε	bed voidage, dimensionless
η	fluid dynamic viscosity, Pa s
ν	fluid kinematic viscosity, m^2/s
ρ	fluid density, kg/m^3

Dimensionless groups

$$j_D = \frac{k_m Sc^{2/3}}{w_0} = \frac{Sh}{Re\, Sc^{1/3}}$$

$$Re = \frac{d_P w_0}{\nu}$$

$$Sc = \frac{\nu}{D_{\mathrm{CO}}}$$

$$Sh = \frac{k_m d_P}{D_{\mathrm{CO}}}$$

Acknowledgments

The authors thank Prof. Michael Türk and Mr. Gerd Upper from the Themodynamic Institute of the University of Karlsruhe for support with the supercritical Pt deposition. This project was financed by the German Research Foundation (DFG) in the frame of the Research Group FOR 583: "Solid Sponges—Application of Monolithic Network Structures in Process Engineering".

References

Buciuman, F.C., Kraushaar-Czarnetzki, B., 2003. Ceramic foam monoliths as catalyst carriers. 1. Adjustment and description of morphology. Industrial Engineering Chemistry Research 42, 1863–1869.

Cybulski, A., Moulijn, J.A., 1994. Monoliths in heterogeneous catalysis. Catalysis Reviews—Science and Engineering 36, 179–270.

Dwivedi, P.N., Upadhyay, S.N., 1977. Particle-fluid mass transfer in fixed and fluidized beds. Industrial and Engineering Chemistry Process Design and Development 16, 157–165.

Giani, L., Groppi, G., Tronconi, E., 2005. Mass-transfer characterization of metallic foams as supports for structured catalysts. Industrial & Engineering Chemistry Research 44, 4993–5002.

Grass, K., Lintz, H.-G., 1995. Tin (IV) oxide supported noble metal catalysts for the carbon monoxide oxidation at low temperatures. In: Poncelet, G., et al. (Eds.), Preparation of Catalysts, vol. VI. Elsevier, Amsterdam, pp. 1111–1119.

Groppi, G., et al., 2006. Monolithic catalysts for gas-phase syntheses of chemicals. In: Cybulski, A., Moulijn, J.A. (Eds.), Structured Catalysts and Reactors, second ed. CRC Taylor & Francis, Boca Raton, pp. 244–310.

Heck, R.M., Gulati, S., Farrauto, R.J., 2001. The application of monoliths for gas phase catalytic reactions. Chemical Engineering Journal 82, 149–156.

Richardson, J.T., Peng, Y., Remue, D., 2000. Properties of ceramic foam catalyst supports: pressure drop. Applied Catalysis A: General 204, 19–32.

Richardson, J.T., Remue, D., Hung, J.K., 2003. Properties of ceramic foam catalyst supports: mass and heat transfer. Applied Catalysis A: General 250, 319–329.

Schryer, D.R., Upchurch, B.T., Sidney, B.D., Brown, K.G., Hoflund, G.B., Herz, R.K., 1991. A proposed mechanism for Pt/SnO_x-catalyzed CO oxidation. Journal of Catalysis 130, 314–317.

Younis, L.B., Viskanta, R., 1993. Experimental determination of the volumetric heat transfer coefficient between stream of air and ceramic foam. International Journal of Heat and Mass Transfer 36, 1425–1434.